frontiers | Frontiers in Chemistry

TYPE Original Research
PUBLISHED 15 September 2022
DOI 10.3389/fchem.2022.995820

OPEN ACCESS

EDITED BY
Wagdy Mohamed Eldehna,
Kafrelsheikh University, Egypt

REVIEWED BY
Ahmed A. Al-Karmalawy,
Horus University, Egypt
Haytham Tawfik,
Tanta University, Egypt

*CORRESPONDENCE
Shahid Iqbal,
shahidgcs10@yahoo.com
Shoaib Khan,
shoaibkhanswati@gmail.com

SPECIALTY SECTION
This article was submitted to Medicinal and Pharmaceutical Chemistry, a section of the journal Frontiers in Chemistry

RECEIVED 19 July 2022
ACCEPTED 17 August 2022
PUBLISHED 15 September 2022

CITATION
Khan Y, Iqbal S, Shah M, Maalik A, Hussain R, Khan S, Khan I, Pashameah RA, Alzahrani E, Farouk A-E, Alahmdi MI and Abd-Rabboh HSM (2022), New quinoline-based triazole hybrid analogs as effective inhibitors of α-amylase and α-glucosidase: Preparation, in vitro evaluation, and molecular docking along with in silico studies.
Front. Chem. 10:995820.
doi: 10.3389/fchem.2022.995820

New quinoline-based triazole hybrid analogs as effective inhibitors of α-amylase and α-glucosidase: Preparation, *in vitro* evaluation, and molecular docking along with *in silico* studies

Yousaf Khan[1], Shahid Iqbal[2]*, Mazloom Shah[3], Aneela Maalik[1], Rafaqat Hussain[4], Shoaib Khan[4]*, Imran Khan[4], Rami Adel Pashameah[5], Eman Alzahrani[6], Abd-ElAziem Farouk[7], Mohammed Issa Alahmdi[8] and Hisham S. M. Abd-Rabboh[9,10]

[1]Department of Chemistry, COMSATS Universityislamabad Campus, Islamabad, Pakistan, [2]Department of Chemistry, School of Natural Sciences (SNS), National University of Science and Technology (NUST), Islamabad, Pakistan, [3]Department of Chemistry, Abbottabad University of Science and Technology (AUST), Abbottabad, Pakistan, [4]Department of Chemistry, Hazara University, Mansehra, Pakistan, [5]Department of Chemistry, Faculty of Applied Science, Umm Al-Qura University, Makkah, Saudi Arabia, [6]Department of Chemistry, College of Science, Taif University, Taif, Saudi Arabia, [7]Department of Biotechnology College of Science, Taif University, Taif, Saudi Arabia, [8]Department of Chemistry, Faculty of Science, University of Tabuk, Tabuk, Saudi Arabia, [9]Chemistry Department, Faculty of Science, King Khalid University, Abha, Saudi Arabia, [10]Department of Chemistry, Faculty of Science, Ain Shams University, Cairo, Egypt

The 7-quinolinyl-bearing triazole analogs were synthesized **(1d–19d)** and further assessed *in vitro* for their inhibitory profile against α-amylase andα-glucosidase. The entire analogs showed a diverse range of activities having IC_{50} values between 0.80 ± 0.05 μM to 40.20 ± 0.70 μM (α-amylase) and 1.20 ± 0.10 μM to 43.30 ± 0.80 μM (α-glucosidase) under the positive control of acarbose (IC_{50} = 10.30 ± 0.20 μM) (IC_{50} = 9.80 ± 0.20 μM**)** as the standard drug. Among the synthesized scaffolds, seven scaffolds **12d**, **10d**, **8d**, **9d**, **11d**, **5d**, and **14d** showed excellent α-amylase and α-glucosidase inhibitory potentials with IC_{50} values of 4.30 ± 0.10, 2.10 ± 0.10, 1.80 ± 0.10, 1.50 ± 0.10, 0.80 ± 0.05, 5.30 ± 0.20, and 6.40 ± 0.30 μM (against α-amylase) and 3.30 ± 0.10, 2.40 ± 0.10, 1.20 ± 0.10, 1.90 ± 0.10, 8.80 ± 0.20, 7.30 ± 0.40, and 5.50 ± 0.10 μM (against α-glucosidase), respectively, while the remaining 12 scaffolds **19d**, **8d**, **17d**, **16d**, **15d**, **7d**, **4d**, **3d**, **1d**, **2d**, **13d** and **6 d** showed less α-amylase and α-glucosidase inhibitory potentials than standard acarbose but still found to be active. Structure–activity connection studies also showed that scaffolds with electron-withdrawing groups like -Cl, $-NO_2$, and -F linked to the phenyl ring had higher inhibitory potentials for -amylase and -glucosidase than scaffolds with $-OCH_3$, -Br, and $-CH_3$ moieties. In order to better understand their binding sites, the powerful scaffolds **11d** and **9d** were also subjected to molecular docking studies. The results showed that these powerful

analogs provide a number of important interactions with the active sites of both of these targeted enzymes, including conventional hydrogen bonding, pi–pi stacking, pi–sulfur, pi–anion, pi–pi, pi–sigma, T-shaped, and halogen (fluorine). Furthermore, various techniques (spectroscopic), including 1H, ^{13}C-NMR, and HREI-MS mass, were used to explore the correct structure of newly afforded hybrid scaffolds based on quinoline-bearing triazole ring.

KEYWORDS

quinoline, triazole, α-amylase enzymes, α-glucosidase enzymes, molecular docking

1 Introduction

In the past few decades, DM (diabetes mellitus) was known to be the most familiar epidemic disorder, which adversely affects the metabolic functions performed by the endocrine system. It is growing and spreading rapidly all over the world. Islets of Langerhans are well-known specialized cells that are responsible for producing insulin in the human body when a diabetic patient does not either produce insulin or is incapable of consuming insulin properly. Due to this dysfunction, the glucose (sugar) level of blood increases in the body, resulting in hyperglycemia. DM is categorized into two types, insulin-reliant, which is due to a lack of production of insulin in the human body termed type-1; however, in type-2 diabetes, either

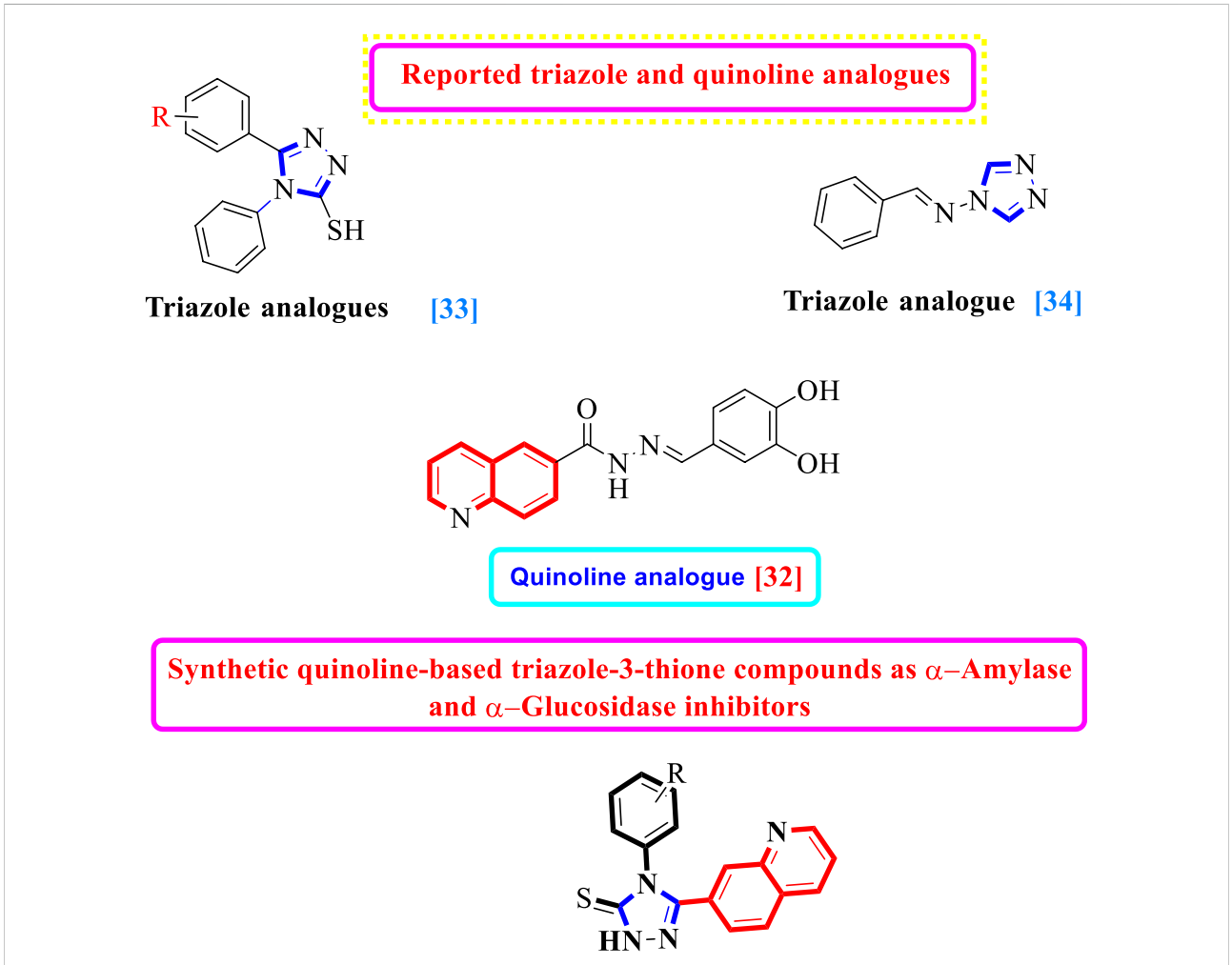

FIGURE 1
Hybridization of the quinoline moiety with a triazole ring.

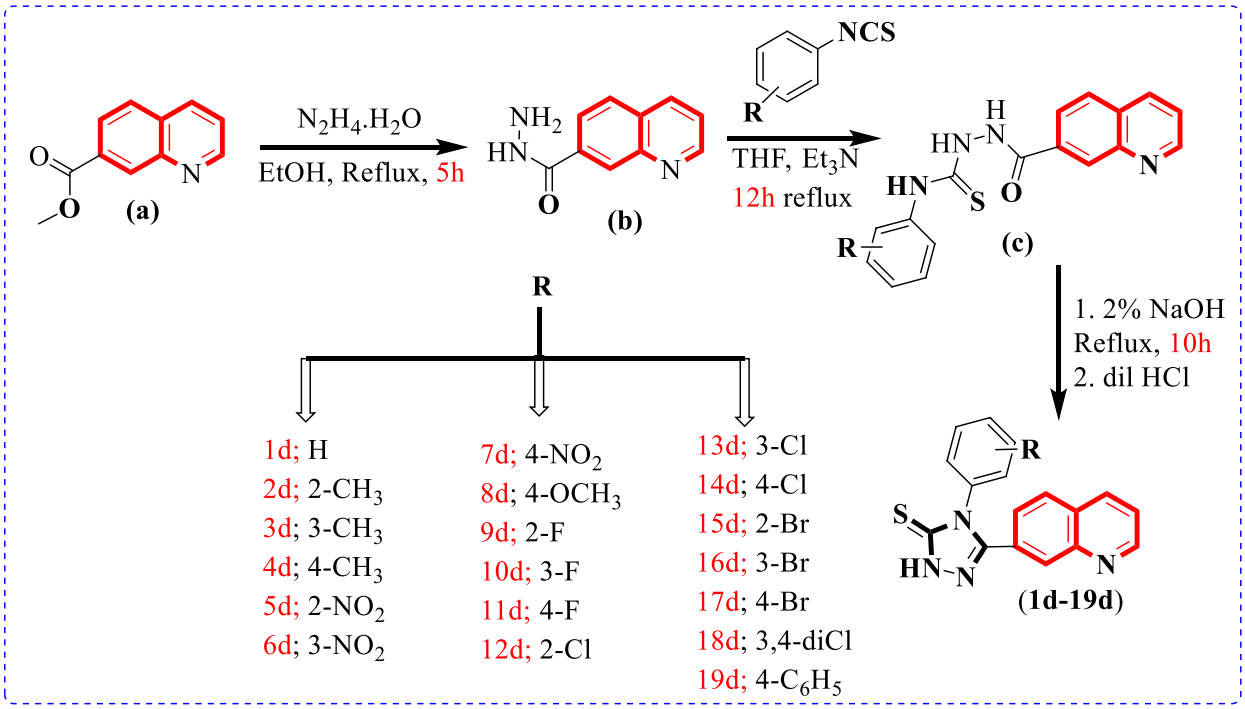

SCHEME 1
Preparation of 7-quinolinyl-based triazole-3-thione derivatives (1d–19d).

TABLE 1 Inhibition profile (*in vitro*) of targeted α-amylase and α-glucosidase enzymes of hybrid scaffolds of quinoline-based triazole (1d–19d).

Synthetic compound	Substituent	IC_{50} ± SEM[a] [μM](α-amylase)	IC_{50} ± SEM[a] [μM](α-glucosidase)
1d	-H	40.20 ± 0.70	43.30±0.80
2d	2-CH_3	22.60 ± 0.60	25.50 ± 0.60
3d	3-CH_3	32.30 ± 0.60	31.60 ± 0.70
4d	4-CH_3	21.60 ± 0.40	22.50±0.40
5d	2-NO_2	5.30 ± 0.20	8.80 ± 0.20
6d	3-NO_2	21.40 ± 0.30	19.50 ± 0.40
7d	4-NO_2	11.60 ± 0.20	14.60 ± 0.30
8d	4-OCH_3	29.40 ± 0.60	32.10 ± 0.60
9d	2-F	1.50 ± 0.10	1.90 ± 0.10
10d	3-F	2.10 ± 0.10	2.40 ± 0.10
11d	4-F	0.80 ± 0.05	1.20 ± 0.10
12d	2-Cl	4.30 ± 0.10	5.50 ± 0.10
13d	3-Cl	14.60 ± 0.30	14.60 ± 0.40
14d	4-Cl	6.40 ± 0.30	7.30 ± 0.40
15d	2-Br	17.20 ± 0.30	19.10 ± 0.20
16d	3-Br	31.80 ± 0.60	33.70 ± 0.60
17d	4-Br	19.20 ± 0.30	23.50 ± 0.40
18d	2,4-diCl	1.80 ± 0.10	3.30 ± 0.10
19d	4-C_6H_5	18.50 ± 0.30	19.30±0.40
Standard acarbose drug	10.30 ± 0.20	9.80 ± 0.20	

TABLE 2 RMSD values of different poses of analog 11d against α-amylase and α-glucosidase enzymes.

Mode	Affinity	Distance from best mode	
	(kcal/mol)	rmsd I.b	rmsd u.b
1	−8.2	0.000	0.000
2	−7.9	2.246	3.655
3	−7.9	3.364	6.471
4	−7.8	2.030	2.595
5	−7.6	3.308	5.323
6	−7.2	3.685	6.603
7	−7.2	3.019	4.418
8	−7.2	4.254	7.764
9	−7.0	2.865	3.903

Analog-5 RMSD values of different poses against alpha-amylase

Mode	Affinity	Distance from best mode	
	(kcal/mol)	rmsd I.b	rmsd u.b
1	−8.5	0.000	0.000
2	−7.7	2.667	3.468
3	−7.3	8.027	10.161
4	−7.0	3.214	5.774
5	−7.0	2.981	5.877
6	−6.8	2.022	2.520
7	−6.8	4.092	5.322
8	−6.8	3.757	6.614
9	−6.6	3.579	5.289

Analog-5 RMSD values of different poses against alpha-glucosidase

TABLE 3 RMSD values of different poses of analog 9d against α-amylase and α-glucosidase enzymes.

Mode	Affinity	Distance from best mode	
	(kcal/mol)	rmsd I.b	rmsd u.b
1	−8.5	0.000	0.000
2	−8.5	2.246	3.435
3	−8.1	3.338	5.131
4	−8.0	3.707	6.835
5	−8.0	3.020	6.097
6	−7.9	2.451	3.725
7	−7.9	3.255	5.056
8	−7.9	2.376	3.374
9	−7.9	5.022	7.801

Analog-5 RMSD values of different poses against alpha-amylase

Mode	Affinity	Distance from best mode	
	(kcal/mol)	rmsd I.b	rmsd u.b
1	−8.6	0.000	0.000
2	−7.6	1.389	1.693
3	−7.5	2.502	3.433
4	−7.4	2.592	3.214
5	−7.3	8.077	9.946
6	−7.0	2.896	3.851
7	−6.9	8.501	10.238
8	−6.7	3.089	5.590
9	−6.7	3.919	6.462

Analog-5 RMSD values of different poses against alpha-glucosidase

insulin is not produced by the human body or is incapable of utilizing insulin properly. After cardiovascular and cancer diseases, which result in mortality, DM is among the most frequent and rapidly growing chronic diseases (Li et al., 2004; Chauhan et al., 2010). However, inhibition of α-amylase and α-glucosidase, as being carbolytic enzymes, is one of the common approaches to minimizing or managing these metabolic disorders (Zaharudin et al., 2019). Lipase, protease, and amylase are the most used enzymes in food biotechnology and industry (Asgher et al., 2007). α-amylase, which belongs to the class of metalloenzymes, catalyzes the formation of glucose and maltose through hydrolysis of starch (polysaccharides) (Sundarram and Murthy, 2014; Taha et al., 2017). The human body absorbs starch through the sequential catalytic action of α-glucosidase (intestinal) andα-amylase (Asgher et al., 2007). Inhibitors of α-amylase and α-glucosidase play a crucial role in modulating the glucose level of blood after taking a meal. Therefore, the α-amylase and α-glucosidase inhibitory potential can be clinically utilized as chemotherapeutic agents and finds applications in the treatment of DM, in addition to obesity (Gunawan-Puteri et al., 2012; Taha et al., 2017).

In addition to the usage of several approaches, the inhibitors of α-glucosidase are used as a therapeutic approach for the treatment of DM (Jong-Anurakkun et al., 2007). The α-glucosidase inhibitors slow down the absorption of glucose, therefore resulting in a decrease in the digestion process. Miglitol and acarbose are important inhibitors of the α-glucosidase enzyme commonly used to decrease the glucose level of postprandial blood. These synthesized inhibitors inhibit glucose formation in the small intestine through inhibition of the α-glucosidase enzyme. Acarbose, an antidiabetic drug with α-amylase and α-glucosidase inhibitory potentials, is currently used in type-2 DM treatment (Salar et al., 2017). Nonetheless, different side effects, such as abdominal pain and flatulence, are associated with acarbose. The use of only drugs is often limited by these side effects; consequently, the efficiency was improved by using in combination with other antidiabetic drugs. Therefore, designing and constructing more active

TABLE 4 RMSD values of different poses of standard acarbose drug against α-amylase and α-glucosidase enzymes.

Mode	Affinity	Distance from best mode	
	(kcal/mol)	rmsd I.b	rmsd u.b
1	−8.0	0.000	0.000
2	−7.8	3.267	11.500
3	−7.8	3.228	10.552
4	−7.7	2.163	9.832
5	−7.5	4.169	7.220
6	−7.5	5.320	9.443
7	−7.4	4.477	8.490
8	−7.4	3.580	11.779
9	−7.2	5.259	9.041

Acarbose RMSD values against alpha-amylase

Mode	Affinity	Distance from best mode	
	(kcal/mol)	rmsd I.b	rmsd u.b
1	−7.3	0.000	0.000
2	−7.3	3.562	11.099
3	−7.3	1.489	2.269
4	−6.9	3.817	10.685
5	−6.9	3.838	10.852
6	−6.7	7.042	13.565
7	−6.7	6.866	11.671
8	−6.6	2.089	11.269
9	−6.6	4.540	11.478

Acarbose RMSD values against alpha-glucosidase

scaffolds having fewer side effects to treat DM is time-consuming (Meneilly et al., 2000).

Quinoline scaffolds find application in numerous pharmaceutically potent drugs and received much attention in the field of medicinal chemistry. Quinoline scaffolds were reported to show a broad range of biological activities such as antifungal (Tabassum et al., 2021), antibacterial (Ghosh et al., 2020), antileishmanial (Gupta et al., 2021), anticonvulsant (Al-Ostoot et al., 2021), anti-Zaka virus (Taha et al., 2019), antimalarial (Vinindwa et al., 2021), proton pump inhibitors (Cernicchi et al., 2021), antiproliferative (Ammar et al., 2021), antiulcer (Atukuri et al., 2020), antidiabetic (Taha et al., 2019), antimicrobial, anti-inflammatory (Douadi et al., 2020), antitrypanosomal (Zhang et al., 2018), antitubercular (Nesaragi et al., 2021), antioxidant agent (Velmurugan et al., 2021), and antihypertensive (Kumari et al., 2019).

It is well known that scaffolds harboring the 1,2,4-triazole motif have a variety of biological and pharmacological properties, including anticonvulsant, anti-inflammatory, antiproliferative, and antifungal activities (Fadaly et al., 2020; Jahani et al., 2020; Joshi et al., 2020). Furthermore, 1,2,4-triazole is a pharmacologically active scaffold that is crucial for therapeutic candidates such as anastrozole, vorozole, and letrozole, all of which have been shown to be efficient aromatase inhibitors and have applications in the treatment of breast cancer (Ammazzalorso et al., 2021). Additionally, it was shown that 1,2,4-triazole containing mercapto scaffolds have antitubercular, antibacterial, antifungal, and anticancer effects (Mallikarjuna et al., 2009; Pitucha et al., 2020).

In the recent past, researchers had investigated numerous heterocyclic moieties of different categories and classes to explore their inhibitory profile in search of lead molecules. Keeping in view the α-amylase and α-glucosidase profile of quinoline and triazole-3-thione analogs, herein in this study, we have incorporated two heterocyclic rings in the same molecule as7-quinolinyl-bearing triazole-3-thione analogs **(1d–19d)** with the hope of further expanding their inhibitory potentials as dual α-amylase and α-glucosidase inhibitors (Figure 1).

2 Results and discussion

2.1 Chemistry

To afford new hybrid scaffolds **(1d–19d)** based on the quinoline-bearing triazole skeleton, methyl quinoline-7-carboxylate (0.5 mmol) (a) solution stirred in EtOH (10 ml) was reacted and refluxed with hydrazine hydrate (1 equivalent) for 5 h. As the reaction was completed, a solid residue (0.5 mmol) was obtained by evaporation of the solvent and then washed with cold water and dried to afford quinoline-7-carbohydrazide (b). In the second step, the mixture of quinoline-7-carbohydrazide (0.5 mmol), the corresponding phenyl isothiocyanates (1 equivalent), and Et_3N (1 ml) in THF (10 ml) was refluxed for 12 h and then quenched with water (10 ml) to form a precipitate, which was further filtered and using EtOH (5 ml) recrystallized to access an intermediate, which further underwent cyclization with 2% NaOH (10 ml) followed by neutralization with dilute HCl (5 ml) to afford the targeted quinoline-based triazole **(1d–19d)** scaffolds in the appropriate yield (Scheme 1) Table 1.

2.2 Biological activity

2.2.1 Inhibition study of α-amylase and α-glucosidase

In this study, nineteen scaffolds based on quinoline-bearing triazole were afforded and then assessed against α-amylase and α-glucosidase to explore their inhibition profile. The entire analogs showed a diverse range of activities having IC_{50} values between 0.80 ± 0.05 μM and 40.20 ± 0.70 μM (α-amylase) and 1.20 ± 0.10 μM and 43.30 ± 0.80 μM (α-glucosidase) under the positive

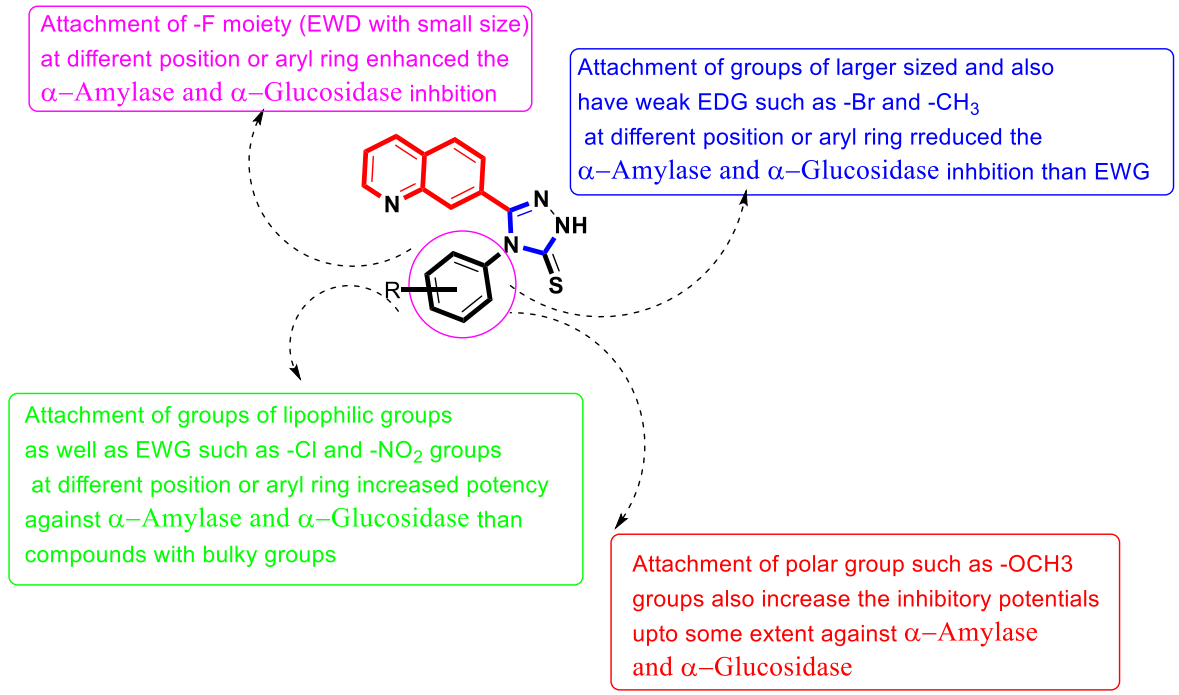

FIGURE 2
Summary of SAR studies of quinoline-based triazole against α-amylase and α-glucosidase enzymes.

control of acarbose [(IC_{50} = 10.30 ± 0.20 μM) (IC_{50} = 9.80 ± 0.20 μM)] as the standard drug. Among the synthesized scaffolds, seven scaffolds **12d**, **10d**, **18d**, **9d**, **11d**, **5d** and **14d** showed superior α-amylase and α-glucosidase inhibitory potentials than standard acarbose drugs with IC_{50} values of 4.30 ± 0.10, 2.10 ± 0.10, 1.80 ± 0.10, 1.50 ± 0.10, 0.80 ± 0.05, 5.30 ± 0.20, and 6.40 ± 0.30 μM (against α-amylase) and 3.30 ± 0.10, 2.40 ± 0.10, 1.20 ± 0.10, 1.90 ± 0.10, 8.80 ± 0.20, 7.30 ± 0.40, and 5.50 ± 0.10 μM (against α-glucosidase), respectively, while the remaining 12 scaffolds **19d**, **8d**, **17d**, **16d**, **15d**, **7d**, **4d**, **3d**, **1d**, **2d**, **13d** and **6d** showed less α-amylase and α-glucosidase inhibitory potentials than standard acarbose but still found to be active. SAR studies suggest that the entire part of synthetic scaffolds, including quinoline, triazole ring, and *N*-phenyl ring, actively participates in the activity, and any change observed in the activity was due to alteration in position, number/s, and nature of substituents around phenyl ring **B**.

2.2.1.1 Structure–activity relationship study for α-amylase enzyme

It was noteworthy from SAR studies that quinoline-based triazole scaffolds that hold the fluoro moiety as being the electron-withdrawing entity attached to various positions of the aryl ring show a significant role in the inhibition of the α-amylase enzyme, and hence hybrid scaffolds based on the quinoline-bearing triazole moiety showed better inhibition than -CH_3, -OCH_3, and–Br groups bearing scaffolds. This enhanced inhibitory potential of fluoro moiety-bearing analogs was due to greater electron withdrawing affinity of the –F moiety, which makes the ph-ring more effective for interactions with α-amylase active pocket. Moreover, it also seemed that the activity was altered by bringing variation in the position of the –F moiety around aryl ring **B**. In current newly afforded scaffolds, the analog **11d** that holds the –F moiety at 4-position of aryl ring **B** linked to the *N*-triazole skeleton was found to show ten-fold enhanced potency than standard acarbose drug. However, analogs **9d** with *ortho*-F and **10d** having *meta*-F substitutions displayed less potency than scaffold **11d**, although these analogs resemble in their structure with analog **9d** but have different positions around phenyl ring **B**. This variation in potency of these–F moiety-bearing scaffolds was due to different positions of the -F moiety at the phenyl ring, indicating that alteration in the position of the –F moiety may result in diverse potency.

Similarly, the alteration in the position of the attached substitute also affects other–Cl moiety-bearing scaffolds **14d**, **12d**, and **13d**. By comparing scaffold **12d** that holds *ortho*–Cl moiety with scaffolds **14d** bearing *para*-Cl and **13d** having *meta*-Cl substitutions, the *ortho*-Cl moiety holding analog **12d** showed enhanced potency than its counterparts **14d** and **13d**, although these scaffolds are structurally similar. This indicates that the activity was diminished by shifting *ortho*-Cl moiety either to

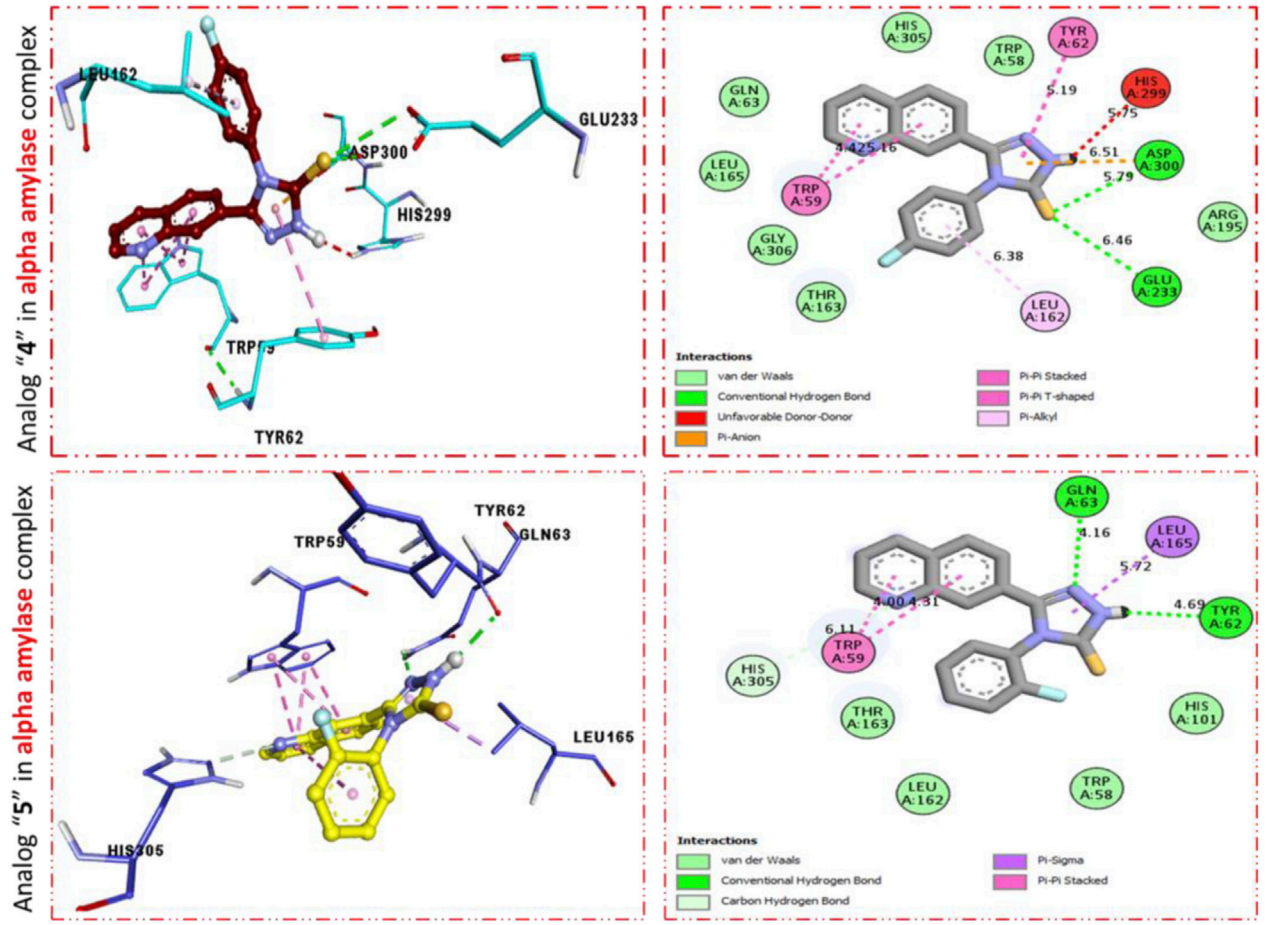

FIGURE 3
PLI profile indicates the corresponding surface of α-amylase enzyme and its interactions with fluoro-substituted scaffolds 11 d and 9d.

para- or *meta*-position as in scaffolds **14d** and **13d**. In addition, compound **14d** bearing *para*-Cl substitution showed 2-folds more potency than scaffold **7d** bearing *para*-NO_2 moieties on the aryl ring, although the position of substituents around the aryl ring is the same. The activity was different in the case of both these compounds, which may be owing to the diverse nature of attached substituents (-Cl and–NO_2). Moreover, by comparing the *ortho*-Cl moiety bearing scaffold **12d** with compound **5d** that hold the *ortho*-NO_2 group on the aryl ring of the triazole skeleton, the scaffold **12d** has emerged as a better inhibitor of α-amylase than scaffold **5d**. This difference in potency between these analogs was caused by the unique properties of both the -Cl and -NO_2 moieties. If we compared compound **14d** (IC_{50} = 6.40 ± 0.30 μM) bearing mono-chloro substitution on *4*-position of the attached *N*-ph-ring with its counterpart 2 bearing di-Cl substitution linked to *3*-and *4*-position of the phenyl ring, the compound **18d** showed better activity than compound **14d** due to the attached di-Cl substitutions that offered stronger electron-withdrawing effect. Analog **1d** having un-substituted attached ph-ring is recognized as the least potent inhibitor among the newly constructed scaffolds. However, the activity may be enhanced when substituents of either electron-withdrawing/electron-donating properties are attached to it at various positions of the ph-ring. Therefore, compounds **8d** (having *para*–OCH_3), **4d** (having *para*–CH_3), **14d** (having (having *para*–Cl), and **18d** (having *3,4*–di-Cl) moieties showed enhanced α–amylase inhibitory potentials when compared to compound **1d** with un-substituted ph-ring, indicating that the activity was largely dependent on attached electron-withdrawing/electron-donating groups (Figure 2).

2.2.1.2 Structure–activity relationship study for α-glucosidase enzyme

Among halogen-substituted analogs, fluoro-substituted analogs (**10d, 11d** and **9d**) showed enhanced α–glucosidase inhibitory potentials when compared to Cl-substituted (**14d**,

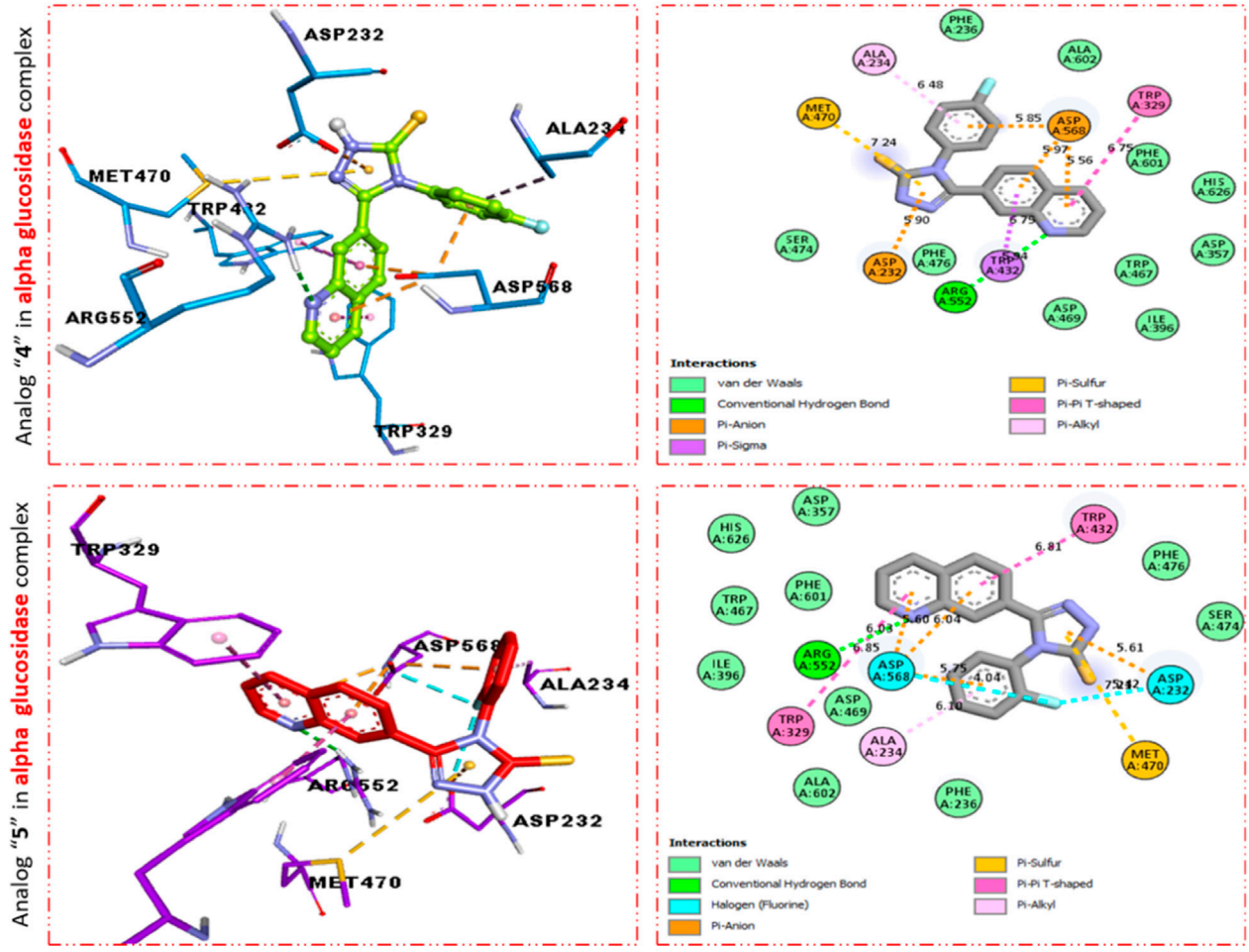

FIGURE 4
PLI profile indicates the corresponding surface of α-glucosidase enzyme and its interactions with fluoro-substituted scaffolds 11 d and 9d.

12d and **13d**) and bromo-substituted analogs (**17d**, **16d** and **15d**). Similarly, Cl-substituted scaffolds display better activity than bromo-substituted analogs. This shows that the α–glucosidase activity was enhanced by increasing the electron-withdrawing nature of the attached substituent; therefore, halogen-substituted scaffolds showed activity in order of–F > Cl > Br. Moreover, by comparing the *para*-F moiety bearing analog **11d** with compounds **10d** bearing *meta*-F and **9d** having *ortho*-F group, compound **11d** showed superior potentials than its counterparts 10d and **9d**, which are similar in structure to compound **11d**. This difference in activity found in these fluoro-substituted analogs was due to the different positions of the attached electron-withdrawing fluoro moiety around the ph-ring. If we compare analog **14d** and **12d** with mono-chloro substitution with compound **18d** bearing 3, 4-di Cl chloro groups, the di-Cl moieties bearing scaffold 18d showed superior activity than a mono-Cl moiety containing scaffolds **14d** and **12d**. This enhanced activity of compound **18d** may be due to the stronger electron-withdrawing effect offered by the two chloro groups as compared to compound **14d** and **12d** bearing mono-chloro substitution. Similarly, by comparing scaffold **5d** bearing *ortho*-nitro substitution with its structurally similar analog **7d** that holds the nitro group at the *para*-position of the phenyl ring, the compound **5d** showed enhanced activity than its counterpart **7d**. This shows that alteration in the position of substitution around the phenyl ring greatly affects the enzymatic activity (Figure 2).

Based on the aforementioned observation, it was concluded that the inhibitory potentials of both α-amylase and α-glucosidase were largely dependent on substitution patterns around the ph-ring attached to the hybrid triazole-based quinoline skeleton. Moreover, it was also noted that the activities changed by bringing alterations in nature, position, and number/s of attached substituents.

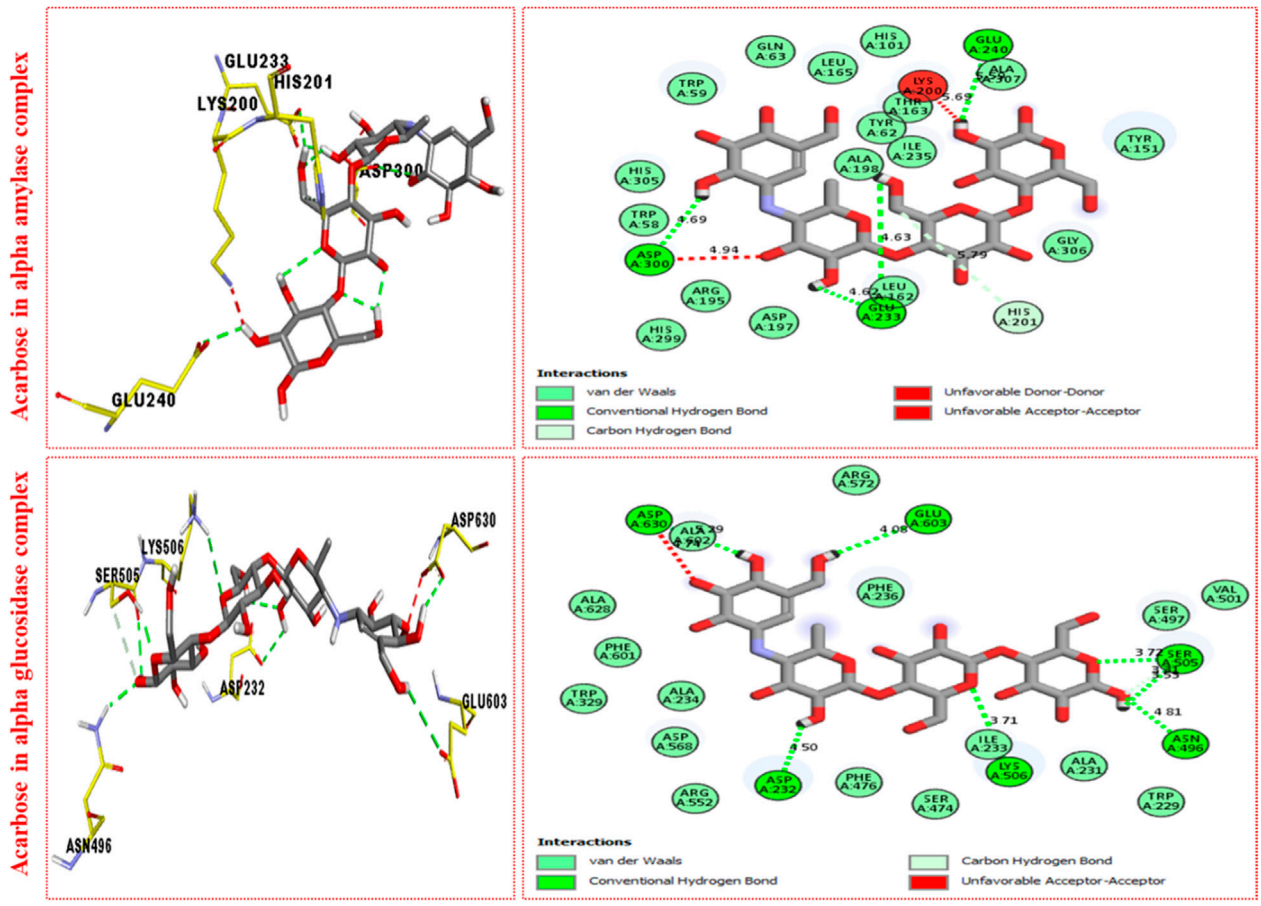

FIGURE 5
PLI profile indicates the corresponding surface of α-amylase and α-glucosidase enzymes and their interactions with the standard acarbose drug.

2.2 Experimental

The experimental data (general procedure, spectral analysis, α-amylase, and α-glucosidase inhibition, and docking protocols (Li et al., 2015; Mrabti, 2018; Rao et al., 2021) were included in the supporting documentation.

3 Molecular docking

To explore the active part in newly constructed quinoline-based triazole scaffolds against α-amylase and α-glucosidase, molecular docking was carried out. Among newly afforded scaffolds being tested, the analogs that hold fluoro moiety showed enhanced inhibitory potentials (*in vitro*), and hence these fluoro-substituted analogs were subjected to the molecular docking study to explore their binding site and results obtained from molecular docking show that the most potent analogs **11d** and **9d** not only display better potency (*in vitro*) but also furnish numerous important interactions (*in silico*) with the active site of the amino acid.

It was shown by the PLI profile of potent analog **11d** bearing–F moiety that analog 11d against α-amylase displays various important interactions (Figure 3) such as TYR-62 (π–π stacked), HIS-299 (donor interactions), ASP-3002 (H-B), GLU-233 (H-B), LEU-162 (π–R), HIS-305 (donor interactions), and TRP-59 (π–π T-shaped). Similarly, analog **9d** in α-amylase showed various interactive residues from a certain distance, while the residues are TRP-59 (π–π stacked), GLN-63 (H-B), LEU-165 (π–sigma), and TRY-62 (H-B) as shown in Figure 3.

Furthermore, scaffold 4 also displays better interactions against the α–glucosidase enzyme. This analog **11d** having *para*-F moiety on the extended aryl ring interacts with α-glucosidase *via* several interactions, including MET-470 (π–S), ALA-234 (π–R), ASP-568 (π–anion), TRP-329 (π–π T-shaped), TRP-432 (π-sigma), ARG-552 (H-B), and ASP-232 (π–anion) as shown in Figure 4, while analog **9d** exhibited the following interactions against alpha glucosidase such as TRP-432 (π–π T-shaped), ASP-232 (H-F), MET-470 (π–S), ALA-234 (π–R), ASP-568 (H-F), TRP-329 (π–π T-Stacked), and ARG-552 (H-B) along with van der Waals interaction (Figure 4).

It was observed by comparison of the protein–ligand interaction profile of most active scaffolds **11d** and **9d** with protein–ligand

interaction of standard acarbose drugs against α-amylase and α-glucosidase enzymes that the active scaffolds **11d** and **9d** established some additional interactions such as halogen (fluorine), π–π T-shaped, π–sulfur, π–alkyl, π–sigma, π–π stacking, and π–anion interactions with the active part of the amino acid of α-amylase and α-glucosidase than standard acarbose drug which furnish only conventional HB van der Waals and carbon HB interactions. Therefore, scaffolds **11d** and **9d** were found to be more potent against α-amylase and α-glucosidase than acarbose standard drugs.

The most potent scaffolds at **11d** and **9d** have different potency (*in vitro*) for both enzymes being targeted and hence established a diverse range of interactions (molecular docking) with active sites of these enzymes (Tables 2–4). This difference in activity and different interactions (*in silico*) possessed by these scaffolds toward enzymes being targeted was due to different positions of the attached fluoro moiety around the aryl part of the quinoline-triazole skeleton. It was shown (Figure 5) from docking results that these potent analogs **11d** and **9d** (possess the–F at a different position) furnish a better binding mode of interactions with the active part of enzymes being targeted (α-amylase and α-glucosidase) than standard acarbose drug which established only conventional HB, van der Waals, and carbon HB interactions with the active part of targeted enzymes (α-amylase and α-glucosidase).

4 Conclusion

In conclusion, the present study synthesized novel hybrid analogs **(1d–19d)** based on a quinoline-bearing triazole moiety in their core structure. The entire constructed analogs were also additionally assessed for α-amylase and α-glucosidase (*in vitro*) inhibitory activities. All scaffolds being synthesized were found to display a diverse range of inhibitory potentials between 0.80 ± 0.05μM and 40.20 ± 0.70 μM (against α-amylase) and 1.20 ± 0.10 μM and 43.30 ± 0.80 μM (against α-glucosidase). Compound **11d** (IC_{50} = 0.80 ± 0.05 μM) (IC_{50} = 1.20 ± 0.10 μM) holding *para*-fluoro substitution on the phenyl ring emerged as the most active analog among the synthesized series. Moreover, compound **9d** with fluoro substitution at the *ortho*-position of the phenyl ring was identified as the second most active analog against α-amylase and α-glucosidase enzymes. Therefore, it was concluded based on SAR studies that scaffolds bearing electron-withdrawing groups such as–NO_2, -Cl, and –F attached to the phenyl ring, resulting in enhanced inhibitory potentials. When these active scaffolds **11d** and **9d** underwent molecular docking analysis, they created a number of significant contacts with the active sites of the two targeted enzymes. The protein–ligand contact profile for compound 11d against α-amylase shows that it established numerous important interactions such as His-305 (donor interactions), Tyr-62 (π–π stacked), His-299 (donor interactions), Asp-3002 (H-B), Glu-233 (H-B), Leu-162 (π–R), and Trp-59 (π–π T-shaped), while against α-glucosidase it also furnishes numerous important interactions, including Met-470 (π-S), Ala-234 (π–R), Asp-568 (π–anion), Trp-329 (π–π T-shaped), Trp-432 (π–sigma), Arg-552 (H-B), and Asp-232 (π–anion). Furthermore, the structures of all the newly synthesized quinoline-based triazole analogs were confirmed by employing different techniques, including ^{1}H NMR, HREI-MS, and ^{13}C-NMRspectroscopy.

Data availability statement

The original contributions presented in the study are included in the article/Supplementary Material; further inquiries can be directed to the corresponding authors.

Author contributions

The manuscript was written with the contributions of all authors. All authors have approved the final version of the manuscript.

Acknowledgments

The authors extend their appreciation to the Deanship of Scientific Research at King Khalid University for funding this work through the General Research Project under grant number (RGP.2/183/43). The authors would like to thank the Deanship of Scientific Research at Umm Al-Qura University for supporting this work by grant code: (22UQU4320141DSR21). Email: rapasha@uqu.edu.sa.

Conflict of interest

The authors declare that the research was conducted in the absence of any commercial or financial relationships that could be construed as a potential conflict of interest.

Publisher's note

Supplementary material

The Supplementary Material for this article can be found online at: https://www.frontiersin.org/articles/10.3389/fchem.2022.995820/full#supplementary-material

References

Al-Ostoot, F. H., Salah, S., and Khanum, S. A. (2021). Recent investigations into synthesis and pharmacological activities of phenoxy acetamide and its derivatives (chalcone, indole and quinoline) as possible therapeutic candidates. *J. Iran. Chem. Soc.* 18 (8), 1839–1875. doi:10.1007/s13738-021-02172-5

Ammar, Y. A., Elhagali, G. A., Abusaif, M. S., Selim, M. R., Zahran, M. A., Naser, T., et al. (2021). Carboxamide appended quinoline moieties as potential anti-proliferative agents, apoptotic inducers and Pim-1 kinase inhibitors. *Med. Chem. Res.* 30 (9), 1649–1668. doi:10.1007/s00044-021-02765-y

Ammazzalorso, A., Gallorini, M., Fantacuzzi, M., Gambacorta, N., De Filippis, B., Giampietro, L., et al. (2021). Design, synthesis and biological evaluation of imidazole and triazole-based carbamates as novel aromatase inhibitors. *Eur. J. Med. Chem.* 211, 113115. doi:10.1016/j.ejmech.2020.113115

Asgher, M., Asad, M. J., Rahman, S. U., and Legge, R. L. (2007). A thermostable α-amylase from a moderately thermophilic Bacillus subtilis strain for starch processing. *J. food Eng.* 79 (3), 950–955. doi:10.1016/j.jfoodeng.2005.12.053

Atukuri, D., Vijayalaxmi, S., Sanjeevamurthy, R., Vidya, L., Prasannakumar, R., and Raghavendra, M. M. (2020). Identification of quinoline-chalcones and heterocyclic chalcone-appended quinolines as broad-spectrum pharmacological agents. *Bioorg. Chem.* 105, 104419. doi:10.1016/j.bioorg.2020.104419

Cernicchi, G., Felicetti, T., and Sabatini, S. (2021). Microbial efflux pump inhibitors: A journey around quinoline and indole derivatives. *Molecules* 26 (22), 6996. doi:10.3390/molecules26226996

Chauhan, A., Sharma, P. K., Srivastava, P., Kumar, N., and Dudhe, R. (2010). Plants having potential antidiabetic activity: A review. *Der Pharm. Lett.* 2 (3), 369–387.

Douadi, K., Chafaa, S., Douadi, T., Al-Noaimi, M., and Kaabi, I. (2020). Azoimine quinoline derivatives: Synthesis, classical and electrochemical evaluation of antioxidant, anti-inflammatory, antimicrobial activities and the DNA/BSA binding. *J. Mol. Struct.* 1217, 128305. doi:10.1016/j.molstruc.2020.128305

Fadaly, W. A., Elshaier, Y. A., Hassanein, E. H., and Abdellatif, K. R. (2020). New 1, 2, 4-triazole/pyrazole hybrids linked to oxime moiety as nitric oxide donor celecoxib analogs: Synthesis, cyclooxygenase inhibition anti-inflammatory, ulcerogenicity, anti-proliferative activities, apoptosis, molecular modeling and nitric oxide release studies. *Bioorg. Chem.* 98, 103752. doi:10.1016/j.bioorg.2020.103752

Ghosh, S., Pal, S., Praveena, K. S. S., and Mareddy, J. (2020). 2-Chloro-7-methyl-3-((4-((p-tolyloxy) methyl)-1H-1, 2, 3-triazol-1-yl) methyl) quinoline: Crystal structure, hydrogen bonding and anti-bacterial activity. *J. Mol. Struct.* 1212, 128137. doi:10.1016/j.molstruc.2020.128137

Gunawan-Puteri, M. D., Kato, E., and Kawabata, J. (2012). α-Amylase inhibitors from an Indonesian medicinal herb, Phyllanthus urinaria. *J. Sci. Food Agric.* 92 (3), 606–609. doi:10.1002/jsfa.4615

Gupta, O., Pradhan, T., Bhatia, R., and Monga, V. (2021). Recent advancements in anti-leishmanial research: Synthetic strategies and structural activity relationships. *Eur. J. Med. Chem.* 223, 113606. doi:10.1016/j.ejmech.2021.113606

Jahani, R., Abtahi, S. R., Nematpour, M., Dastjerdi, H. F., Chamanara, M., Hami, Z., et al. (2020). Design, synthesis, and pharmacological evaluation of novel 1, 2, 4-triazol-3-amine derivatives as potential agonists of GABAA subtype receptors with anticonvulsant and hypnotic effects. *Bioorg. Chem.* 104, 104212. doi:10.1016/j.bioorg.2020.104212

Jong-Anurakkun, N., Bhandari, M. R., and Kawabata, J. (2007). α-Glucosidase inhibitors from Devil tree (Alstoniascholaris). *Food Chem.* 103 (4), 1319–1323. doi:10.1016/j.foodchem.2006.10.043

Joshi, R., Kumari, A., Singh, K., Mishra, H., and Pokharia, S. (2020). Triorganotin (IV) complexes of Schiff base derived from 1, 2, 4-triazole moiety: Synthesis, spectroscopic investigation, DFT studies, antifungal activity and molecular docking studies. *J. Mol. Struct.* 1206, 127639. doi:10.1016/j.molstruc.2019.127639

Kumari, L., Mazumder, A., Pandey, D., Yar, M. S., Kumar, R., Mazumder, R., et al. (2019). Synthesis and biological potentials of quinoline analogues: A review of literature. *Mini. Rev. Org. Chem.* 16 (7), 653–688. doi:10.2174/1570193x16666190213105146

Li, W. L., Zheng, H. C., Bukuru, J., and De Kimpe, N. (2004). Natural medicines used in the traditional Chinese medical system for therapy of diabetes mellitus. *J. Ethnopharmacol.* 92 (1), 1–21. doi:10.1016/j.jep.2003.12.031

Li, Z., Gu, J., Zhuang, H., Kang, L., Zhao, X., and Guo, Q. (2015). Adaptive molecular docking method based on information entropy genetic algorithm. *Appl. Soft Comput.* 26, 299–302. doi:10.1016/j.asoc.2014.10.008

Mallikarjuna, B. P., Sastry, B. S., Kumar, G. S., Rajendraprasad, Y., Chandrashekar, S. M., and Sathisha, K. (2009). Synthesis of new 4-isopropylthiazole hydrazide analogs and some derived clubbed triazole, oxadiazole ring systems–A novel class of potential antibacterial, antifungal and antitubercular agents. *Eur. J. Med. Chem.* 44 (11), 4739–4746. doi:10.1016/j.ejmech.2009.06.008

Meneilly, G. S., Ryan, E. A., Radziuk, J., Lau, D. C., Yale, J. F., Morais, J., et al. (2000). Effect of acarbose on insulin sensitivity in elderly patients with diabetes. *Diabetes care* 23 (8), 1162–1167. doi:10.2337/diacare.23.8.1162

Mrabti, N. N. (2018). QSAR study and molecular docking of benzimidazole derivatives inhibitors of p38 kinase. *Moroc. J. Chem.* 6 (3), 6–3. doi:10.48317/IMIST.PRSM/morjchem-v6i3.9273

Nesaragi, A. R., Kamble, R. R., Bayannavar, P. K., Shaikh, S. K. J., Hoolageri, S. R., Kodasi, B., et al. (2021). Microwave assisted regioselective synthesis of quinoline appended triazoles as potent anti-tubercular and antifungal agents via copper (I) catalyzed cycloaddition. *Bioorg. Med. Chem. Lett.* 41, 127984. doi:10.1016/j.bmcl.2021.127984

Pitucha, M., Janeczko, M., Klimek, K., Fornal, E., Wos, M., Pachuta-Stec, A., et al. (2020). 1, 2, 4-Triazolin-5-thione derivatives with anticancer activity as CK1γ kinase inhibitors. *Bioorg. Chem.* 99, 103806. doi:10.1016/j.bioorg.2020.103806

Rao, C. M. M. P., Naidu, N., Priya, J., Rao, K. P. C., Ranjith, K., Shobha, S., et al. (2021). Molecular docking and dynamic simulations of benzimidazoles with beta-tubulins. *Bioinformation* 17 (3), 404. doi:10.6026/97320630017404

Salar, U., Khan, K. M., Chigurupati, S., Taha, M., Wadood, A., Vijayabalan, S., et al. (2017). New hybrid hydrazinyl thiazole substituted chromones: As potential α-amylase inhibitors and radical (DPPH & ABTS) scavengers. *Sci. Rep.* 7 (1), 16980–17017. doi:10.1038/s41598-017-17261-w

Sundarram, A., and Murthy, T. P. K. (2014). α-Amylase production and applications: A review. *J. Appl. Environ. Microbiol.* 2 (4), 166–175. doi:10.12691/jaem-2-4-10

Tabassum, R., Ashfaq, M., and Oku, H. (2021). Current pharmaceutical aspects of synthetic quinoline derivatives. *Mini Rev. Med. Chem.* 21 (10), 1152–1172. doi:10.2174/1389557520999201214234735

Taha, M., Javid, M. T., Imran, S., Selvaraj, M., Chigurupati, S., Ullah, H., et al. (2017). Synthesis and study of the α-amylase inhibitory potential of thiadiazole quinoline derivatives. *Bioorg. Chem.* 74, 179–186. doi:10.1016/j.bioorg.2017.08.003

Taha, M., Sultan, S., Imran, S., Rahim, F., Zaman, K., Wadood, A., et al. (2019). Synthesis of quinoline derivatives as diabetic II inhibitors and molecular docking studies. *Bioorg. Med. Chem.* 27 (18), 4081–4088. doi:10.1016/j.bmc.2019.07.035

Velmurugan, K., Don, D., Kannan, R., Selvaraj, C., VishnuPriya, S., Selvaraj, G., et al. (2021). Synthesis, antibacterial, anti-oxidant and molecular docking studies of imidazoquinolines. *Heliyon* 7 (7), e07484. doi:10.1016/j.heliyon.2021.e07484

Vinindwa, B., Dziwornu, G. A., and Masamba, W. (2021). Synthesis and evaluation of Chalcone-Quinoline based molecular hybrids as potential anti-malarial agents. *Molecules* 26 (13), 4093. doi:10.3390/molecules26134093

Zaharudin, N., Staerk, D., and Dragsted, L. O. (2019). Inhibition of α-glucosidase activity by selected edible seaweeds and fucoxanthin. *Food Chem.* 270, 481–486. doi:10.1016/j.foodchem.2018.07.142

Zhang, H., Collins, J., Nyamwihura, R., Ware, S., Kaiser, M., and Ogungbe, I. V. (2018). Discovery of a quinoline-based phenyl sulfone derivative as an antitrypanosomal agent. *Bioorg. Med. Chem. Lett.* 28 (9), 1647–1651. doi:10.1016/j.bmcl.2018.03.039